NANO LETTERS

Letter

pubs.acs.org/NanoLett

Robust and Multifunctional Nanosheath for Chemical and Biological Nanodevices

Hyun-Wook Ra,[†,∥,⊥] Jin-Tae Kim,[†,⊥] Rizwan Khan,[†] Deepti Sharma,[†] Yeong-Geun Yook,[†] Yoon-Bong Hahn,[†] Jin-Ho Park,[‡] Dae-Ghon Kim,[§] and Yeon-Ho Im*[,†]

[†]School of Semiconductor and Chemical Engineering, [‡]College of Veterinary Medicine, and [§]Medical School, Chonbuk National University, Baekje-Daero, Deokjin-Gu, Jeonju, Jeonbuk 561-756, South Korea

Supporting Information

ABSTRACT: The contribution of advanced nanoscale chemical and biological devices to life science has been limited to a small number of nanomaterials, due to the absence of effective surface modification routes. Herein, we demonstrate a polymer-like nanosheath synthesized by nonthermal plasma technology (NPT) that can protect the core nanomaterial from the solution environment and provide a multifunctional platform for chemical and biological nanosensors. For ZnO nanowires (NWs) which are unstable in solution, we demonstrate that this nanosheath makes it possible for ZnO NW field-effect transistors to act as a pH sensor for 24 h and a biosensor for the real-time, label-free detection of liver cancer markers.

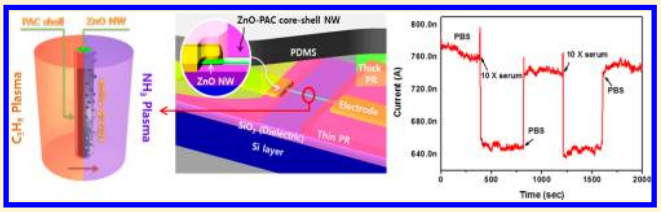

KEYWORDS: *Nanosheath, ZnO nanowire, polymer-like amorphous carbon, ZnO-PAC core−shell, AFP, liver cancer*

Nanoscale chemical and biological sensors are emerging as one of the most impressive platforms for the specific identification of biomolecules and chemical species in the life sciences, with the nanotechnology revolution up to the scale in concert with biological systems.[1,2] Among the various approaches to nanoscale biosensors, field effect transistors (FETs) using semiconductor nanowires (NWs) have been demonstrated to be outstanding platforms for the real-time, label-free, highly sensitive, and multiplexed detection of biological and chemical species.[1,3,4] The sensing principle of NW-based FETs is based on the monitoring of the conductance change resulting from the specific binding of a charged species to the surface of the nanostructure. Although various NW-based materials could be applied to this paradigm, silicon (Si) NWs are well placed to achieve this purpose on account of their controllable size and electronic properties and wide range of available information about the chemical modification of their surfaces.[1,3,4]

One of the promising materials for NW-based FET biosensors is zinc oxide (ZnO), due to its unique optical, electrical, mechanical, chemical, and n-type semiconductor properties,[5,6] which can provide a large variety of novel applications by the coupling of these properties, such as piezoelectric FET,[7] optomechanical devices,[8] optoelectronic devices,[9] and chemical and biological sensors.[10,11] Furthermore, it can be used to create a wide range of nanostructures, including NWs, nanobelts, nanotetrapods, and nanosheets, by relatively easy, cheap, and safe synthesis routes, leading to fascinating platforms for use in nanoscale sensor applications.[5,6,12,13] The additional benefit of ZnO NWs is an oxide semiconductor with good stability in an air environment, as compared to that of nonoxide semiconductor, such as Si NWs. For example, it may be desirable to remove native oxide on the Si NWs by a harsh wet etching process, in order to achieve more effective surface modification platforms with optimization of chemical and biological NW sensors.[14,15] In spite of these advantages, the use of ZnO nanostructures in chemical and biological sensing applications has not been successful, due to their inherent drawbacks related to their chemical instability in liquid solution.[11,16]

Herein, we demonstrate a robust and multifunctional nanosheath based on nonthermal plasma technology, which can overcome the problem of the chemical instability of the core ZnO NWs in a solution environment and make it possible for them to serve as pH sensors and biosensors. As shown in Figure 1a, the NPT-based chemical modifications on the surface of the synthesized ZnO NWs were performed by the deposition of polymer-like amorphous carbon (PAC) and the subsequent formation of amino groups for the effective immobilization of biomolecules. The transmission electron microscopy (TEM) image in Figure 1b shows a single ZnO NW surrounded uniformally by a PAC shell with a thickness of approximately 5.5 nm. The corresponding selected area electron diffraction (SAED) analysis is shown in the inset of Figure 1b, indicating that the ZnO NW in the core region with a diameter of ∼100 nm is able to retain its single-crystal structure of hexagonal wurtzite without any damage or contamination after the formation of the PAC shell by NPT. As shown in Figure 1c, the synthesis of the ZnO-PAC core−shell NWs (ZnO/PAC NWs) is confirmed by the wide scan X-

Received: December 5, 2011
Revised: February 24, 2012
Published: March 20, 2012

dx.doi.org/10.1021/nl204280d | *Nano Lett.* 2012, 12, 1891−1897

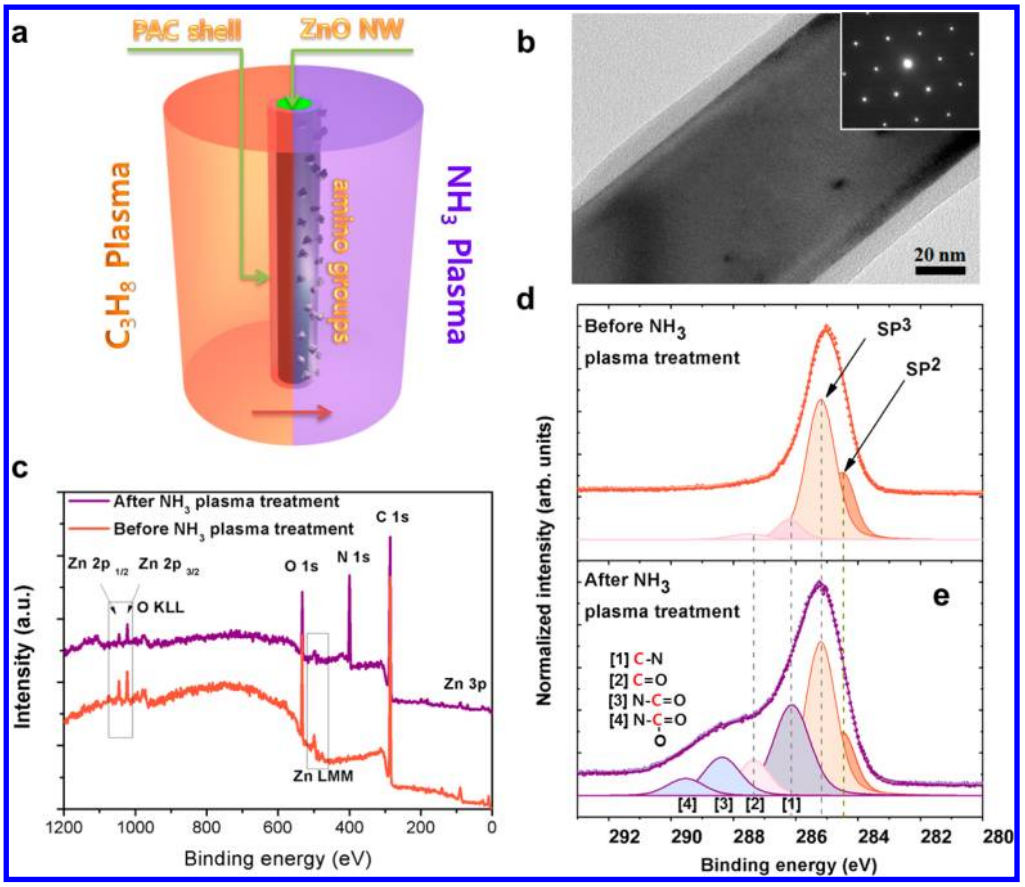

Figure 1. Synthetic method and characterizations of amino functionalized ZnO/PAC NW. (a) Schematic illustration of sequential processes used to form the PAC shell (orange, C_3H_8 plasma) and amino groups on its surface (violet, NH_3 plasma) outside the ZnO NW by nonthermal plasma technology. (b) TEM image of the ZnO/PAC NW. The inset is the corresponding SAED pattern of the ZnO NW. (c) Wide scan XPS spectrum from the ZnO/PAC NWs before and after the NH_3 plasma treatment. (d) The deconvoluted XPS spectrum of the C 1s energy region obtained from the ZnO/PAC NWs before and after the NH_3 plasma treatment.

ray photoelectron spectra (XPS), which present the chemical compositions before and after the chemical surface modifications. Furthermore, this approach allows the thickness of the PAC shell on the ZnO NWs to be controlled up to a few nanometers without any significant changes in the electrical properties of the ZnO NWs, as reported in our previous work.[17]

As shown in Figure 1a, we employed stepwise functionalization procedures for the immobilization of the biomolecules (biotin or anti-α-feptoprotein (AFP) antibody) on the ZnO NWs using plasma polymerization and NH_3 (or O_2) plasma treatment. First, the ZnO/PAC NWs were fabricated by sequential thermal evaporation and plasma enhanced chemical vapor deposition (PECVD), as reported elsewhere.[17] Briefly, the ZnO NWs were synthesized on the Si substrate by thermal evaporation using Zn powders at 900 °C for 30 min in a horizontal tube furnace. Then, the PAC shell was created on the as-synthesized ZnO NWs on the Si substrate using propane (C_3H_8) plasma deposition at room temperature for 10 min in a 13.56 MHz radio frequency (RF)-PECVD system. The key process parameters for the formation of the PAC shell are as follows: C_3H_8/Ar flow rate of 40/4 sccm, chamber pressure of 100 mTorr, and RF power of 300 W. To fabricate the NW FETs or nanosensors, the ZnO/PAC NWs were immersed in ethanol solution and dispersed by sonication. The ZnO/PAC NW FETs or nanosensors can be formed by the conventional electric-field-assisted assembly between two predefined Ti (10 nm)/Au (10 nm) electrodes.[17,18] The top contact electrodes of Ti (40 nm)/Au (60 nm) were deposited on the substrate with aligned ZnO/PAC NWs after O_2 plasma ashing at 100 W for 100 s to remove the outer PAC shell near the metal contact (refer to the white circle inserted in Figure 2a). For the formation of amino groups on the ZnO/PAC NW surface, NH_3 plasma treatment was carried out in a 13.56 MHz RF-inductively coupled plasma (ICP) system. The key parameters are as follows: NH_3 flow rate of 50 sccm, chamber pressure of 100 mTorr, source power of 200 W, no bias power, and plasma treatment time of 5 min.

For the immobilization of the anti-AFP antibody, the ZnO/PAC NWs were dipped in a solution of the anti-AFP monoclonal antibody (10 μg/mL in phosphate buffered saline (PBS) at pH 7.4, AbFrontier) for 12 h at room temperature. To study the orientation of the anti-AFP antibody on the ZnO/PAC NWs, the sandwich binding method was adopted in this work.[19] In this approach, a solution of the AFP antigen (10 μg/mL in PBS at pH 7.4, AbDserotec) and serum of a liver carcinoma patient (diluted 10× in PBS at pH 7.4, Chonbuk National University Hospital) was reacted with the anti-AFP modified ZnO/PAC NWs for 12 h at room temperature. Then, these samples were dipped in a solution of the anti-AFP polyclonal antibody labeled with tetramethyl rhodamine isothiocyanate (TRITC, 10 μg/mL in PBS at pH 7.4) for 12 h at room temperature. After the immobilization of the AFP antibody−antigen, the unbound species were removed by

dx.doi.org/10.1021/nl204280d | *Nano Lett.* 2012, 12, 1891−1897

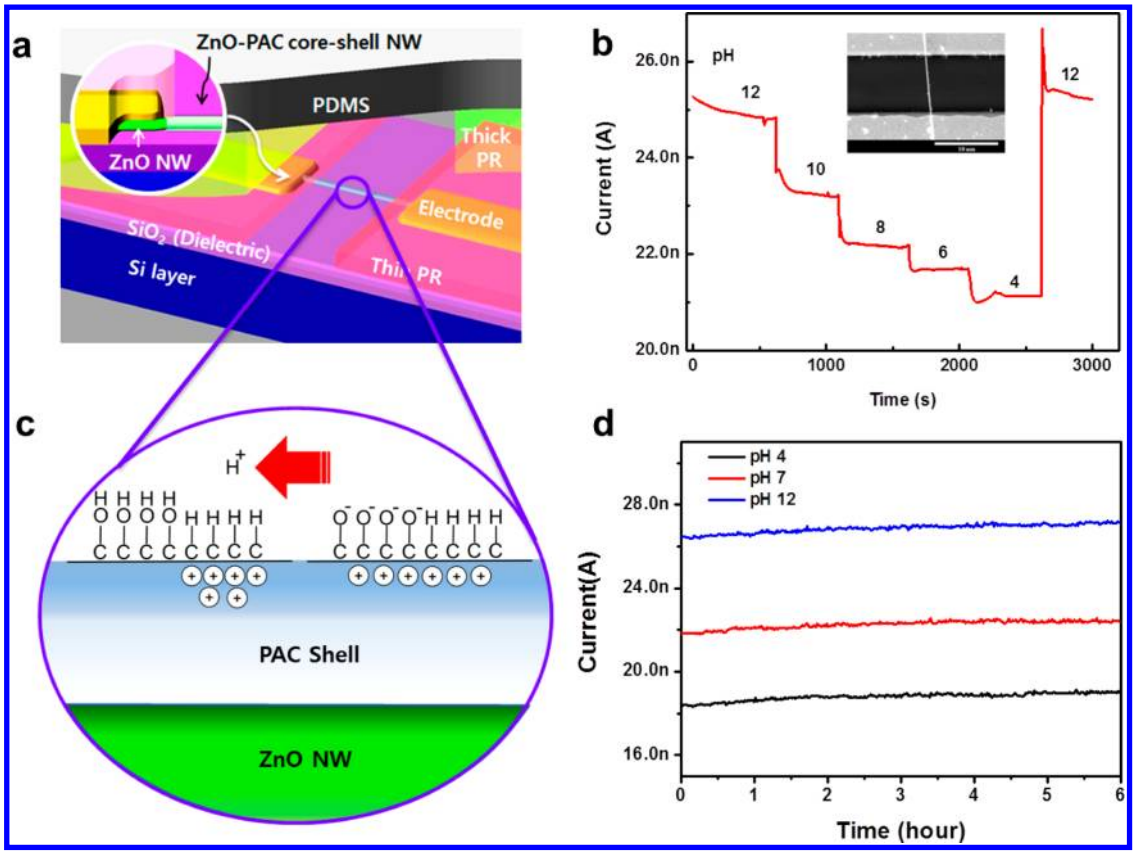

Figure 2. pH detection characteristics from an individual ZnO/PAC NW nanosensor. (a) Schematic illustrating the ZnO/PAC NW nanosensor integrated with a microfluid channel. The enlarged white circle illustrates the metal contact with the ZnO NW after the removal of the PAC shell. (b) Real-time responses of ZnO/PAC NW with different pH values ranging from 4 to 12. The PAC surface is partially oxidized by the oxygen plasma treatment. The inset is the FESEM image of a typical NW device. (c) Schematic view of the enlarged NW surface illustrating the variation of the distribution of holes on the partially oxidized PAC surface with the pH. (d) The response of an individual ZnO/PAC NW FET to different pH buffer solutions for 6 h.

rinsing thoroughly with PBS. The fluorescence microscopy data were collected using a conventional confocal fluorescence microscopy with a 10 mW He−Ne laser excitation emission for the generation of a wavelength of 543 nm, which is suitable for TRITC.

For the fabrication of the effective NW-based biosensor, its surface should be modified chemically with functional groups, such as CHO, NH_2, and SH, in order for it to be able to bind biological molecules. For example, the Si NWs with their natural oxide layer could utilize the extensive data from wet chemical modification of glass surfaces with the conventional self-assembly monolayer (SAM) for biological sensors.[1,20] Unfortunately, these approaches are not the best alternative for ZnO NWs which are unstable in aqueous solution during wet chemical modification. Even after careful surface modification with conventional SAMs, it was observed that the ZnO NWs could not be protected from acid/base solutions, because their surfaces were only partially covered with the SAMs and, therefore, still reacted with the solution (ref 21, Figure S1, Supporting Information).

As part of our effort to address this challenging issue, we formed a PAC shell on the unstable ZnO NWs to protect them from aqueous solutions, in order to be able to use them in the field of chemical and biological sensor applications. The PAC shell in our approach consists of a polymer-like structure in which the carbon atoms are sp^2-and sp^3-hybridized (284.5 and 285.2 eV, respectively),[22] as shown in the deconvoluted XPS C 1s spectra (Figure 1d). Considering only the relative ratio of the sp^2 and sp^3 bondings, the proportion of sp^3-hybridized carbon atoms in the PAC shell is around 70%, which is close to that of diamond-like amorphous carbon. Furthermore, the PAC material can be easily incorporated with the conventional SAM technique, because its surface can support the effective adsorption sites with hydrophilic groups (OH and NH_2) by subsequent processes using various approaches.[23−25] For example, subsequent NH_3 plasma treatment on the surface of the PAC shell can be an effective method of creating amino groups, as shown in Figure 1c,e. The C 1s peak shows that sp^3 C−N bondings related to amino groups were created on the surface of PAC shell after the NH_3 plasma treatment (Figure 1e). It is noted that the small oxygen-related peaks in the XPS analysis are most likely due to the natural oxidation of the dangling bonds on the surface in air (Figure 1d,e).

As shown in Figure 2a, the chemically modified ZnO NW is positioned between the predefined metal electrodes by conventional electric-field-assisted assembly.[18] Before forming the top contact metal electrodes with good ohmic contacts, the PAC shell at the contact position was removed by oxygen plasma treatment, as shown inside the white circle inserted in Figure 2a. Then, a thin photoresist (PR) layer was patterned on the metal electrode to prevent electrochemical reactions between the metal electrodes and solution. The microfluidic channel for the transport of the sample solutions was fabricated using thick PR (150 μm) and polydimethylsiloxane (PDMS)

dx.doi.org/10.1021/nl204280d | *Nano Lett.* 2012, 12, 1891−1897

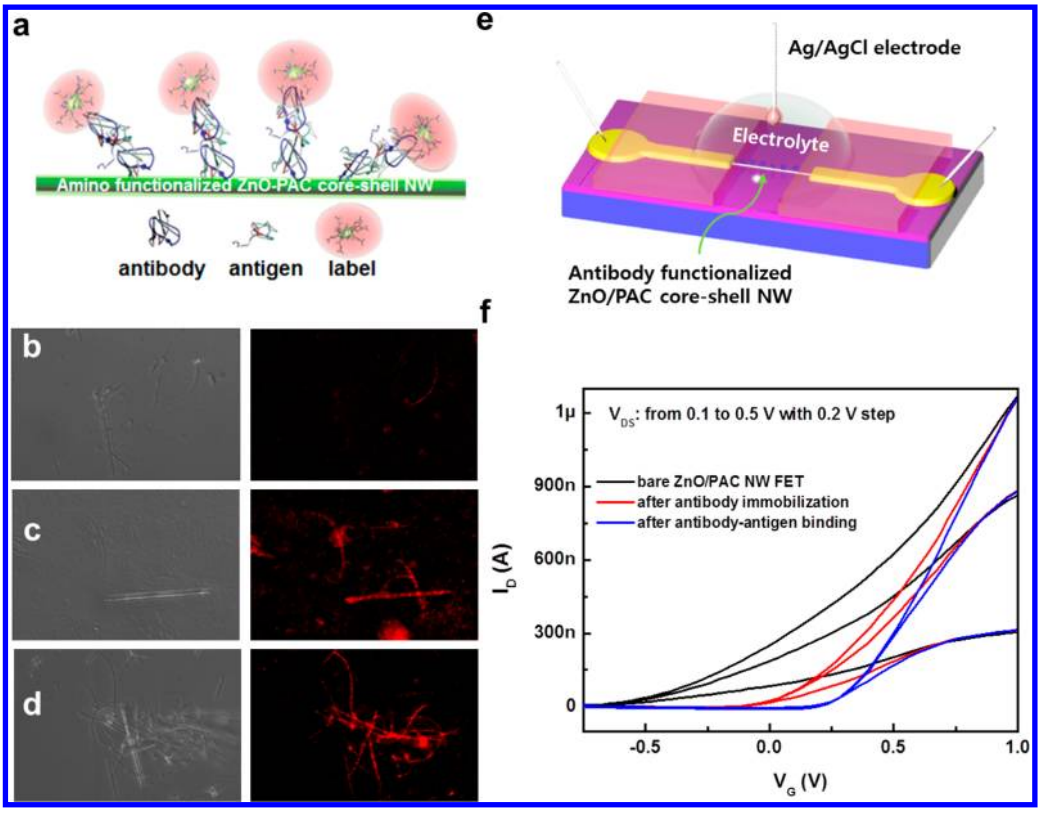

Figure 3. AFP bioimmobilization and electrical characterization of amino functionalized ZnO/PAC NW. (a) Schematic diagram of the sandwich binding method used to examine the AFP immobilization and antibody orientations. After the sandwich binding of the anti-AFP antibody labeled with TRITC immobilization, the fluorescence microscopy images of the (b) untreated ZnO/PAC NW using AFP antigen, (c) amino functionalized ZnO/PAC NW using AFP antigen, and (d) amino functionalized ZnO/PAC NW using the serum of a liver carcinoma patent instead of the AFP antigen. (e) Schematic illustrating electrolyte-gated ZnO/PAC NW FET for electrical characterization. (f) Transfer characteristics of the electrolyte-gated ZnO/PAC NW FET according to AFP-related biomolecules immobilizations. The current level of the NW FET is higher than that of pH detection (Figure 2) due to multiple ZnO NWs between two electrodes.

(Figure 2a). We were able to measure the conductance of the ZnO/PAC NW under the continuous flow of different pH solutions. It was found that the untreated and amino functionalized ZnO/PAC NWs are insensitive to changes in the pH. However, the NW shows clear pH sensitivity (Figure 2b) after modifying the PAC shell with C−O bonds by means of oxygen plasma treatment. It was observed that the current under a constant source−drain voltage (1.7 V) decreases stepwise with decreasing pH from 12 to 4 with significant changes in each step. Furthermore, the current recovers up to its original level with increasing pH from 4 to 12, indicating that the modified NWs can function as a reversible pH sensor.

The basic pH sensing mechanism in conventional ion-sensitive field effect transistors (ISFETs) with an insulator (oxide)/semiconductor structure has been explained by the site-binding model in which the semiconductor is directly affected by the surface charge according to the ion adsorption/desorption (H^+ and OH^-) on the oxidized insulator surface.[26] However, our result in Figure 2b clearly shows that the current of the core ZnO NW with n-type semiconductor characteristics decreases with decreasing pH from 12 to 4, despite the increase of the positive gating effect near the surface of the ZnO-PAC NW. To explain the reverse response, Figure 2c shows a magnified view of the oxygen plasma treated NW in solutions with different pH values. The PAC surface would be expected to be composed of partially O- and H-terminated carbon surfaces, due to the oxygen plasma treatment of the ZnO/PAC NW, as shown in Figure 2c. First, the H-terminated part of the PAC shell in water solution can cause the accumulation of holes, due to electron transfer from the PAC shell surface to the solution. This behavior is known to be the origin of the p-type conductive layer in a hydrogenated diamond surface with mostly sp^3 carbon bonds, which is similar to the H-terminated surface of the PAC shell in this work.[27,28] As the solution pH decreases, the O-terminated surface on the PAC shell changes from negatively charged groups (C−O^-) to a neutral surface or positively charged groups (C−OH or C−OH_2^+), because of the increase of the adsorbed protons at the O-terminated surface. Then, the accumulation of holes underneath the H-terminated surface would be expected to become more pronounced with the increase in the number of positively charged groups on the O-terminated surface, leading to the suppression of the current flow in the core ZnO NW. In contrast, the accumulation of holes is alleviated with increasing pH, as shown in Figure 2c, so that the current flow in the core ZnO NW increases. Although further studies are required to obtain a complete understanding of these phenomena, we believe that this can explain why the opposite response is observed in this study, as compared to that of conventional ISFETs.

As shown in Figure 2d, it is surprising that the electrical signals of the ZnO NW in the solutions with different pHs were quite stable for almost 24 h in our experiments, considering the previously reported instability of ZnO NWs in solution.[16] This result was confirmed by additional experiments which show that the PAC coating prevents the ZnO NWs thin film from completely reacting with acid and base solutions (Figure S1,

dx.doi.org/10.1021/nl204280d | *Nano Lett.* 2012, 12, 1891−1897

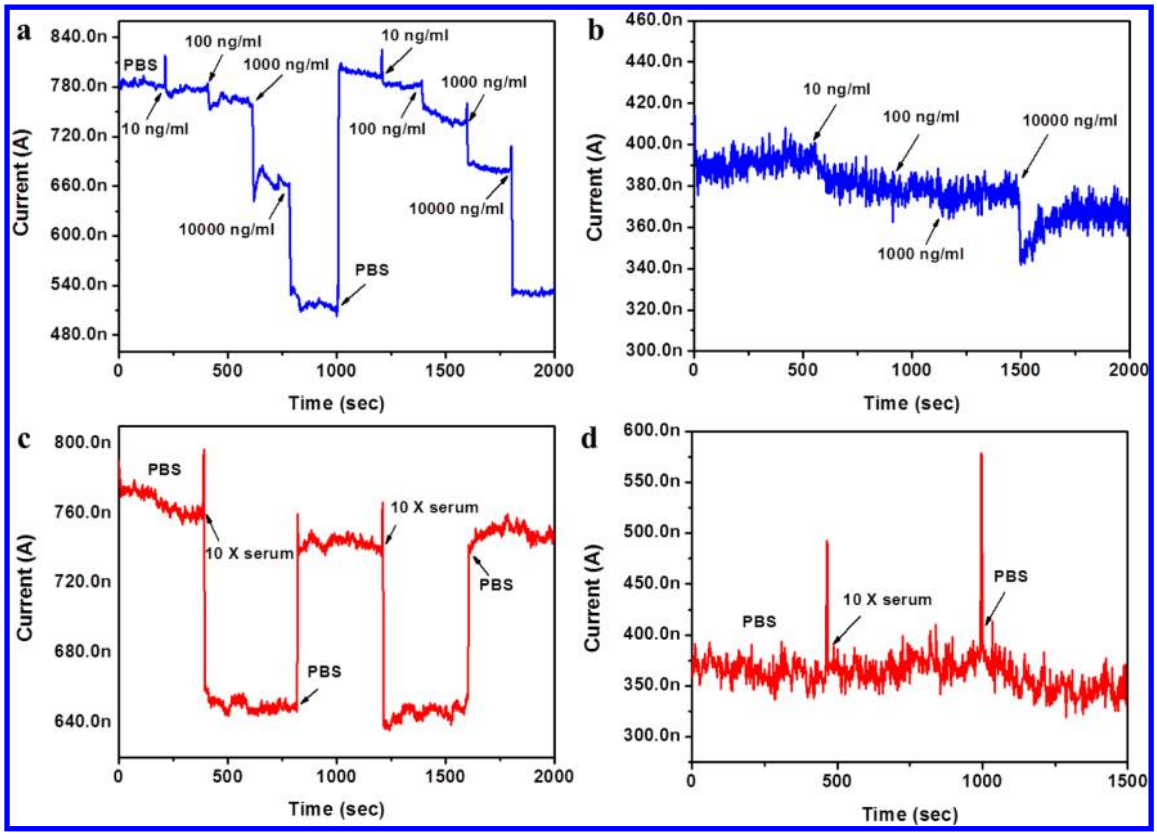

Figure 4. Reversible real-time detection of liver carcinoma biomarker. Time dependence for the response of the ZnO/PAC NW nanosensor with and without anti-AFP antibody immobilizaition (a,b) according to the variation of the concentration of the AFP antigen in 10 mM PBS buffer at pH 7.2. Time dependence for the response of the ZnO/PAC NW nanosensor with and without anti-AFP antibody immobilizaition (c,d) for the serum of a liver carcinoma patient in 10 mM PBS buffer at pH 7.2.

Supporting Information). This can also be regarded as a predictable result based on a previous report that PAC thin films similar to those in our study can play the role of a gas barrier in gas permeation experiments.[29] In other words, our surface modification platform of the conventional NWs can provide a novel biosensing environment without any interaction of the semiconductor NW with the solution. In addition, we demonstrated that widely available inorganic layers, such as the conventional Al_2O_3 ALD layers, are not suitable as insulators for chemical and biological NW sensors with robust solution stability, due to the amphoteric nature and aqueous permeability of this material (Figure S2, Supporting Information). To confirm the potential biosensor applications of our approach, it was demonstrated that the amino functionalized ZnO/PAC NW FETs could be directly employed for the real-time detection of strong ligand−receptor bindings, such as biotin−streptavidin and biotin−avidin, which have commonly been used to characterize conventional NW FET biosensors (Figure S3, Supporting Information).[1,20]

Based on the above studies, the ZnO NW biosensor with NPT-based chemical modifications was applied to the real-time, label-free detection of AFP, which is a representative hepatocellular cancer (HCC) marker in the conventional immunoassay to date.[19,30] The AFP is negatively charged at neutral pH due to its isoelectric point of 4.4−4.9, and its binding with the monoclonal antibody is weak enough to lead to reversible detections due to its dissociation constant of $\sim 10^{-8}$ M.[19,31] To elucidate the inherent characteristics of the PAC shell for biosensor applications, the immobilization of the anti-AFP monoclonal antibody using noncovalent (electrostatic and/or van der Waals) binding was performed for both the amino terminated and untreated ZnO/PAC NWs, without introducing any SAM for the purpose of covalent binding and steric stabilization. The orientation of the anti-AFP antibody to the target NWs was investigated by a sandwich assay method with high reliability (Figure 3a). Based on the fluorescence microscopy images (Figure 3b,c), it was found that the binding of the labeled secondary antibody with the AFP antigen occurs mostly in the case of the NWs with the amino functionalized PAC shell (Figure 3c) as compared to the untreated PAC shell with the mostly hydrogen terminated surface (Figure 3b). In other words, these results demonstrate that the orientation of primary anti-AFP antibody in terms of its antigen binding is better on the amino functionalized surface than on the hydrogen terminated surface. According to a previous work, the physisorbed orientation of specific antibody (e.g., IgG1) is improved on an NH_2 terminated SAM surface as compared to a COOH or CH_3 terminated SAM surface.[32] The surface orientation of the anti-AFP molecules observed in this study is similar to that in previous works, indicating that the amino functionalized PAC shell can be an effective platform for HCC biosensor applications. Figure 3d presents the fluorescence microscopy image of the sandwich assay for the amino functionalized NWs using the serum of a liver carcinoma patient instead of pure AFP antigen, leading to the same result as that in Figure 3c.

The electrical properties of the ZnO/PAC NW before and after the immobilization of the AFP-related biomolecule were measured using the electrolyte-gated NW FETs, as shown in Figure 3e. The NW FET was immersed in an electrolyte drop

dx.doi.org/10.1021/nl204280d | *Nano Lett.* 2012, 12, 1891−1897

(PBS buffer) with an Ag/AgCl electrode as the top gate to minimize the environmental effects of the electrolyte solution. Figure 3f represents the typical transfer characteristics of the amino functionalized NW FET before and after the immobilization of the AFP biomolecule (black and red lines). In all cases, the NW FET before and after the immobilization of the AFP-related biomolecule exhibits typical n-type semiconducting behavior, according to the applied electrolyte gate voltage (V_G). After the immobilization of the anti-AFP antibody, it was observed that the drain current (I_D) decreases, while the threshold voltage shifts positively, due to the adsorption of the negatively charged anti-AFP antibody on the NW surface. After adding the AFP antigen to the anti-AFP antibody modified NW FET, the drain current and threshold voltage decrease and shift positively, respectively (blue lines), suggesting that the net charge of the AFP antigen is negative.

The ZnO/PAC NW FET immobilized with the anti-AFP antibody was applied to the real-time, label-free detection of the AFP antigen fed through a microfluidic channel (Figure S4, Supporting Information). It is known that the average concentration of AFP is typically 5−15 ng/mL in healthy human serum and increases to greater than 500 ng/mL in the serum of liver carcinoma patients.[30] Figure 4a represents the reversible response of the NW FET with the variation of the concentration of the AFP antigen in the range from 10 to 10 000 ng/mL in 10 mM PBS at pH 7.2. The current in the ZnO core NW decreased with increasing concentration of AFP antigen and recovered to the initial value upon its subsequent exposure to 10 mM PBS buffer at pH 7.2. The decrease in the current of the ZnO NW is most likely due to the negatively charged AFP antigen over the PAC shell, as described in Figure 3f. Moreover, the restoration of the current upon the removal of the AFP antigen solution indicates the existence of a reversible binding reaction due to the weak affinity of the AFP antibody−antigen, as described previously. Figure 4b shows the typical response of the ZnO/PAC NW FET without the immobilized anti-AFP antibody according to the variation of the AFP antigen concentration in 10 mM PBS buffer at pH 7.2. In this case, there were no significant changes in the current for various concentrations of the AFP antigen, indicating that the current changes observed for the NW FET with the immobilized anti-AFP antibody correspond to the specific binding of the AFP antibody−antigen. For a concentration of the AFP antigen of 10 μg/mL, it is noted that a slight decrease in the current occurs due to the physisorption of the AFP antigen.

Based on the above observation, the anti-AFP modified NW FET was applied to the real-time, label-free detection of the serum of a liver carcinoma patient diluted up to 10× with 10 mM PBS at pH 7.2. Figure 4c,d represents the real-time responses for the serum of the liver carcinoma patient from the ZnO/PAC NW FET with and without the immobilized anti-AFP antibody, respectively. It was revealed that the anti-AFP antibody modified ZnO/PAC NW FET makes it possible to achieve the real-time, reproducible detection of the AFP antigen from the serum of the liver carcinoma patient (Figure 4c). On the other hand, Figure 4d shows that the ZnO/PAC NW FET without the immobilized anti-AFP antibody does not lead to any significant current changes, regardless of the presence or absence of the serum of the liver carcinoma patient. These results suggest that the ZnO/PAC NW FET can be applied successfully to the real-time, label-free detection of cancer biomarkers in human serum. Furthermore, this platform can be directly extended to high-performance biosensor applications with higher sensitivity and selectivity, since the PAC shell can be easily functionalized with conventional SAMs for the purpose of covalent binding and steric stabilization.

In summary, we demonstrated an NPT-based surface modification route that can provide a robust and multifunctional nanosheath for chemical and biological nanodevices. The PAC nanosheath was synthesized without any significant changes in the chemical structure and electrical properties of the NW material in the core region. Based on ZnO NW FET with solution instability, it was concluded that the inherent characteristics of the PAC nanosheath could provide multifunctional platform for chemical and biological applications in various aspects of solution permeability, electrochemical properties in solution, and biomolecule immobilization via additional functionization. Finally, we demonstrated the use of the ZnO/PAC NW FET as a pH sensor for 24 h and a biosensor for the real-time, label-free detection of the HCC marker in human serum.

■ ASSOCIATED CONTENT

Supporting Information

Details concerning additional results for the chemical stability of the pristine and functionalized ZnO NWs in wet solution, long-term stability of Al_2O_3 ALD layer coated ZnO NW sensors, streptavidin and avidin detection of biotin modified ZnO/PAC NW sensor, and experimental setup including the completed ZnO/PAC NW device images. This material is available free of charge via the Internet at http://pubs.acs.org.

■ AUTHOR INFORMATION

Corresponding Author

*E-mail: yeonhoim@jbnu.ac.kr.

Present Address

[‖]Samsung Electronics, Banwol-Dong, Hwasung-City, Gyeonggi-Do 445−701, South Korea

Author Contributions

[⊥]These authors contributed equally to this work.

Notes

The authors declare no competing financial interest.

■ ACKNOWLEDGMENTS

This work was supported by a National Research Foundation of Korea (NRF) grant funded by the Korea government (MES) (2010-0013234). This study was also supported by the Ministry for Health, Welfare, and Family affairs (A101834), Republic of Korea. The authors wish to thank S. W. Kim (Daewoo Industry R&D center) for the artwork and H. J. Yun (Korea Basic Science Institute) for his assistance in the XPS analysis.

■ REFERENCES

(1) Cui, Y.; Wei, Q. Q.; Park, H. K.; Lieber, C. M. *Science* **2001**, *293* (5533), 1289−1292.

(2) Bangar, M. A.; Shirale, D. J.; Chen, W.; Myung, N. V.; Mulchandani, A. *Anal. Chem.* **2009**, *81* (6), 2168−2175.

(3) Zheng, G. F.; Patolsky, F.; Cui, Y.; Wang, W. U.; Lieber, C. M. *Nat. Biotechnol.* **2005**, *23* (10), 1294−1301.

(4) Stern, E.; Vacic, A.; Rajan, N. K.; Criscione, J. M.; Park, J.; Ilic, B. R.; Mooney, D. J.; Reed, M. A.; Fahmy, T. M. *Nat. Nanotechnol.* **2010**, *5* (2), 138−142.

(5) Huang, M. H.; Mao, S.; Feick, H.; Yan, H. Q.; Wu, Y. Y.; Kind, H.; Weber, E.; Russo, R.; Yang, P. D. *Science* **2001**, *292* (5523), 1897−1899.

(6) Pan, Z. W.; Dai, Z. R.; Wang, Z. L. *Science* **2001**, *291* (5510), 1947−1949.
(7) Wang, X. D.; Zhou, J.; Song, J. H.; Liu, J.; Xu, N. S.; Wang, Z. L. *Nano Lett.* **2006**, *6* (12), 2768−2772.
(8) Gao, P.; Wang, Z. Z.; Liu, K. H.; Xu, Z.; Wang, W. L.; Bai, X. D.; Wang, E. G. *J. Mater. Chem.* **2009**, *19* (7), 1002−1005.
(9) Law, M.; Greene, L. E.; Johnson, J. C.; Saykally, R.; Yang, P. D. *Nat. Mater.* **2005**, *4* (6), 455−459.
(10) Choi, A.; Kim, K.; Jung, H. I.; Lee, S. Y. *Sens. Actuators, B* **2010**, *148* (2), 577−582.
(11) Yeh, P. H.; Li, Z.; Wang, Z. L. *Adv. Mater.* **2009**, *21* (48), 4975−4978.
(12) Greene, L. E.; Law, M.; Tan, D. H.; Montano, M.; Goldberger, J.; Somorjai, G.; Yang, P. D. *Nano Lett.* **2005**, *5* (7), 1231−1236.
(13) Ra, H. W.; Choi, K. S.; Hahn, Y. B.; Im, Y. H. *J. Phys. Chem. C* **2008**, *112* (46), 17926−17930.
(14) Park, I.; Li, Z. Y.; Pisano, A. P.; Williams, R. S. *Nanotechnology* **2010**, *21* (1), 015501.
(15) Haick, H.; Hurley, P. T.; Hochbaum, A. I.; Yang, P. D.; Lewis, N. S. *J. Am. Chem. Soc.* **2006**, *128* (28), 8990−8991.
(16) Zhou, J.; Xu, N. S.; Wang, Z. L. *Adv. Mater.* **2006**, *18* (18), 2432−2435.
(17) Ra, H. W.; Choi, D. H.; Kim, S. H.; Im, Y. H. *J. Phys. Chem. C* **2009**, *113* (9), 3512−3516.
(18) Ra, H. W.; Choi, K. S.; Ok, C. W.; Jo, S. Y.; Bai, K. H.; Im, Y. H. *Appl. Phys. Lett.* **2008**, *93* (3), 033112.
(19) Jang, J. S.; Kim, J. M.; Chung, G. H.; Paik, B. H.; Kim, H. J. *J. Biochem. Mol. Biol.* **1996**, *29* (3), 192−199.
(20) Stern, E.; Klemic, J. F.; Routenberg, D. A.; Wyrembak, P. N.; Turner-Evans, D. B.; Hamilton, A. D.; LaVan, D. A.; Fahmy, T. M.; Reed, M. A. *Nature* **2007**, *445* (7127), 519−22.
(21) Wirth, M. J.; Fairbank, R. W. P.; Fatunmbi, H. O. *Science* **1997**, *275* (5296), 44−47.
(22) Retzko, I.; Unger, W. E. S. *Adv. Eng. Mater.* **2003**, *5* (7), 519−522.
(23) Muguruma, H. *Plasma Processes Polym* **2010**, *7* (2), 151−162.
(24) Lockett, M. R.; Shortreed, M. R.; Smith, L. M. *Langmuir* **2008**, *24* (17), 9198−9203.
(25) Sun, B.; Colavita, P. E.; Kim, H.; Lockett, M.; Marcus, M. S.; Smith, L. M.; Hamers, R. J. *Langmuir* **2006**, *22* (23), 9598−9605.
(26) James A. Davis, R. O. J.; James O, Leckie *J. Colloid Interface Sci.* **1998**, *63* (3), 480−499.
(27) Maier, F.; Riedel, M.; Mantel, B.; Ristein, J.; Ley, L. *Phys. Rev. Lett.* **2000**, *85* (16), 3472−3475.
(28) Garrido, J. A.; Hardl, A.; Kuch, S.; Stutzmann, M.; Williams, O. A.; Jackmann, R. B. *Appl. Phys. Lett.* **2005**, *86* (7), 073504.
(29) Ogino, A.; Nagatsu, M. *Thin Solid Films* **2007**, *515* (7−8), 3597−3601.
(30) Johnson, P. J.; Poon, T. C. W.; Hjelm, N. M.; Ho, C. S.; Blake, C.; Ho, S. K. W. *Br. J. Cancer* **2000**, *83* (10), 1330−1337.
(31) Aoyagi, Y.; Ikenaka, T.; Ichida, F. *Cancer Res.* **1979**, *39* (9), 3571−4.
(32) Chen, S. F.; Liu, L. Y.; Zhou, J.; Jiang, S. Y. *Langmuir* **2003**, *19* (7), 2859−2864.